

# Photochemical modelling in the Po basin with focus on formaldehyde and ozone

L. Liu<sup>1,2</sup>, F. Flatøy<sup>3</sup>, C. Ordóñez<sup>4</sup>, G. O. Braathen<sup>1</sup>, C. Hak<sup>5</sup>, W. Junkermann<sup>6</sup>, S. Andreani-Aksoyoglu<sup>4</sup>, J. Mellqvist<sup>7</sup>, B. Galle<sup>7</sup>, A. S. H. Prévôt<sup>4</sup>, and I. S. A. Isaksen<sup>2</sup>

<sup>1</sup>Norwegian Institute for Air Research, Kjeller, Norway

<sup>2</sup>University of Oslo, Meteorology and Oceanography Section, Department of Geosciences, Oslo, Norway

<sup>3</sup>Bjerknes Centre for Climate Research, University of Bergen, Bergen, Norway

<sup>4</sup>Laboratory of Atmospheric Chemistry, Paul Scherrer Institut, Villigen, Switzerland

<sup>5</sup>Institute of Environmental Physics, Heidelberg, University of Heidelberg, Germany

<sup>6</sup>Research Centre Karlsruhe, Institute for Meteorology and Climate Research, Garmisch Partenkirchen, Germany

<sup>7</sup>Department of Radio and Space, Chalmers University of Technology, Göteborg, Sweden

Received: 30 January 2006 – Published in Atmos. Chem. Phys. Discuss.: 21 June 2006

Revised: 22 November 2006 – Accepted: 8 December 2006 – Published: 11 January 2007

**Abstract.** As part of the EU project FORMAT (Formaldehyde as a Tracer of Oxidation in the Troposphere), a field campaign was carried out in the vicinity of Milan during the summer of 2002. Results from a 3-D regional chemical transport model (NILU RCTM) were used to interpret the observations focusing primarily on HCHO and ozone. The performance of the model was assessed by comparing model results with ground based and aircraft measurements. The model results show good agreement with surface measurements, and the model is able to reproduce the photochemical episodes during fair weather days. The comparison indicates that the model can represent well the HCHO concentrations as well as their temporal and spatial variability. The relationship between HCHO and ( $O_3 \times H_2O$ ) was used to validate the model ability to predict the HCHO concentrations. Further analysis revealed the importance of the representativeness of different instruments: in-situ concentrations might be locally enhanced by emissions, while long path measurements over a forest can be influenced by rapid formation of HCHO from isoprene. The model is able to capture the plume from the city of Milan and the modelled levels agree generally well with the aircraft measurements, although the wind fields used in the model can lead to a displacement of the ozone plume. During the campaign period,  $O_3$  levels were seldom higher than 80 ppb, the peak surface ozone maxima reached 90 ppb. Those relatively low values can be explained by low emissions during the August vacation and unstable weather conditions in this period. The modelled  $\Delta O_3/\Delta NO_z$  slope at Alzate of 5.1 agrees well with the measured slope of 4.9.

## 1 Introduction

Ozone ( $O_3$ ) is harmful both to humans and vegetation, and the extent of damage depends on the concentration of ozone and the duration of exposure (Heck et al., 1982; Gong et al., 1986). The surface ozone levels at European rural and remote sites have increased by more than a factor of two from the beginning of the industrialization (Volz and Kley, 1988; Anfossi et al., 1991; Marenco et al., 1994; Staehelin et al., 1994; Pavelin et al., 1999) because of the large increase in the emissions of ozone precursors during this period. Ozone builds up to toxic levels in the atmosphere during warm, sunny weather when pollutants, mainly nitrogen oxides ( $NO_x=NO+NO_2$ ), CO and volatile organic compounds (VOCs), accumulate in stagnant air. Ozone levels in polluted areas can be elevated to more than 100 ppb in a few days under favourable weather conditions (e.g. Isaksen et al., 1978; Prévôt et al., 1997). Many regulations have been applied to reduce ozone levels in the last decades, but the improvements are limited, especially for the rural areas (Solberg et al., 2004, 2005; Ordóñez et al., 2005). This is because the ozone production is highly non-linear and controlled by VOC, CO and  $NO_x$ . The ozone production per unit  $NO_x$  depends on the VOC/ $NO_x$  ratio, VOC reactivity and the  $NO_x$  levels (Isaksen et al., 1978; Liu et al., 1987; Lin et al., 1988). Besides the influence of anthropogenic emissions of ozone precursors, highly reactive biogenic emissions, especially of isoprene, add uncertainties to the ozone production and distribution both in urban and rural areas (Trainer et al., 1987; Chameides et al., 1988).

Formaldehyde is the most abundant carbonyl compound in the atmosphere. It can be directly emitted from incomplete combustion processes, or produced by photooxidation of hydrocarbons. The direct emissions mostly come from

Correspondence to: L. Liu  
(lil@geo.uio.no)

biomass burning or combustion engines. Precursor hydrocarbons, which give rise to secondary formaldehyde, also have many different anthropogenic and biogenic sources. The formaldehyde concentration level varies from several tens of pptv in clean background air, to tens of ppb in hydrocarbon rich air. As an intermediate in the oxidation of hydrocarbons to carbon monoxide (CO), HCHO plays an important role in the hydrocarbon oxidation chain and the CO budget. Through photolysis and reaction with the hydroxyl radical (OH), HCHO acts as an important source for the hydroperoxyl radical ( $\text{HO}_2$ ), which leads to ozone production when  $\text{NO}_x$  is present. Because of its widespread presence and its role in photooxidation, HCHO is a key component for local, regional and large-scale photochemical processes and budgets.

Accurate measurements of HCHO are therefore important for the understanding of odd hydrogen species (OH and  $\text{HO}_2$ ), ozone production and global CO budget. Highly sensitive techniques are required to measure HCHO under different circumstances. HCHO measurements were performed in several projects in the last two decades (e.g. Harris et al., 1989; Heikes et al., 1996; Hov and Flatøy, 1997), and differences between various types of HCHO measurements were found (Gilpin et al., 1997; Cárdenas et al., 2000). These discrepancies were considered to be caused by different techniques, or by the instruments setup. One of the main objectives of the FORMAT project was to gain a better understanding of the disagreement between different measurement techniques. Hence, an intensive comparison between different in-situ measurement methods was performed during the 2002 campaign in the Po Basin. The results indicate that there is a good agreement between different techniques as long as the same air mass is measured, and that the observed disagreements are mainly caused by different instrument setups (Hak et al., 2005).

The Milan metropolitan area has a population of about 4 million and is the most industrialized and populated area in northern Italy. Episodes with high photooxidant levels are frequently observed in this region. In previous campaigns in the Po Basin, such as the POLLUMET campaign in 1992 and the PIPAPO campaign in 1998,  $\text{O}_3$  mixing ratios up to 185 ppb and 190 ppb were measured, respectively (Prévôt et al., 1997; Neftel et al., 2002; Dommen et al., 2002; Thielmann et al., 2002). These studies focused on the ozone production and VOC/ $\text{NO}_x$  sensitivity. Both measurements and the model results concluded that the ozone production is VOC limited within the Milan plume, and  $\text{NO}_x$  limited in the surroundings. The previous studies show that the highest  $\text{O}_3$  levels are mostly found in VOC controlled regimes, approximately 30 km downwind of the emission sources (Prévôt et al., 1997; Martilli et al., 2002; Thielmann et al., 2002; Baertsch-Ritter et al., 2003, 2004; Andreani-Aksoyoglu et al., 2004). HCHO is present in high concentrations in this area as well, directly emitted (mainly from vehicles) or produced from oxidation of hydrocarbons. Typical levels about

10 ppb and a peak value up to 33 ppb were observed in the summer month, downwind of the Milan metropolitan area (Staffelbach et al., 1997; Aliche et al., 2002).

To achieve the goal of improved air quality, better scientific tools for understanding and reproducing the photochemical smog episodes are needed. Many comprehensive numerical models have been developed to simulate the photochemical processes in Europe. In addition to supply scientific support to emission abatement, numerical models can also be used for the forecasting of air pollution events. Tilmes et al. (2002) evaluated five Eulerian state-of-the-art chemical transport models including NILU RCTM, and concluded that the most comprehensive models give the best results. The NILU RCTM has been used in several European Union projects (TACIA, ACSOE, POLINAT, MAXOX, INCA, ACTO), which involved aircraft measurements. The model provided chemical forecasts for the planning of the flight routes (Flatøy et al., 2000). During the FORMAT campaign the model was used for the same purpose. The model results were evaluated with various measurements from surface and aircraft, and show a good ability to reproduce the photochemical evolution present in the measurements. In this paper, based on the intensively measured HCHO dataset, a more detailed model evaluation is presented. With a better understanding of discrepancies between different HCHO measurement techniques, the model performance has been evaluated against the observations. For the first time, this model has been used to interpret the photochemical evolution in a very polluted region with complex terrain.

## 2 The FORMAT 2002 campaign

### 2.1 Time period and measurement platforms

The campaign was carried out in the Po Basin, Italy from 22 July to 20 August 2002. The Po Basin was chosen for the FORMAT campaign in order to capture the photochemical transformation of the Milan photooxidation plume, and to achieve a better understanding of the evolution of formaldehyde and its role in a highly polluted area.

During the campaign ground-based measurements of HCHO and additional species were carried out at two sites located in the north of Milan city (Fig. 1). The site at Alzate, used as a semi-rural station, is located downwind and about 35 km north of Milan, close to the foothills of the Alps, and 404 m a.s.l. The other site, at Bresso, is an urban station in the northern outskirts of Milan city, also downwind, but influenced by direct emissions from the city. For a detailed description of Alzate and Bresso see Thielmann et al. (2002).

An ultralight aircraft operated by IMK-IFU carried out airborne measurements during the campaign. The aircraft was based at the airfield of Lecco Monte Marenzo, a small airport located 10 km south of Lecco and about 35 km north-east of Milan. The typical flight routes covered regions north

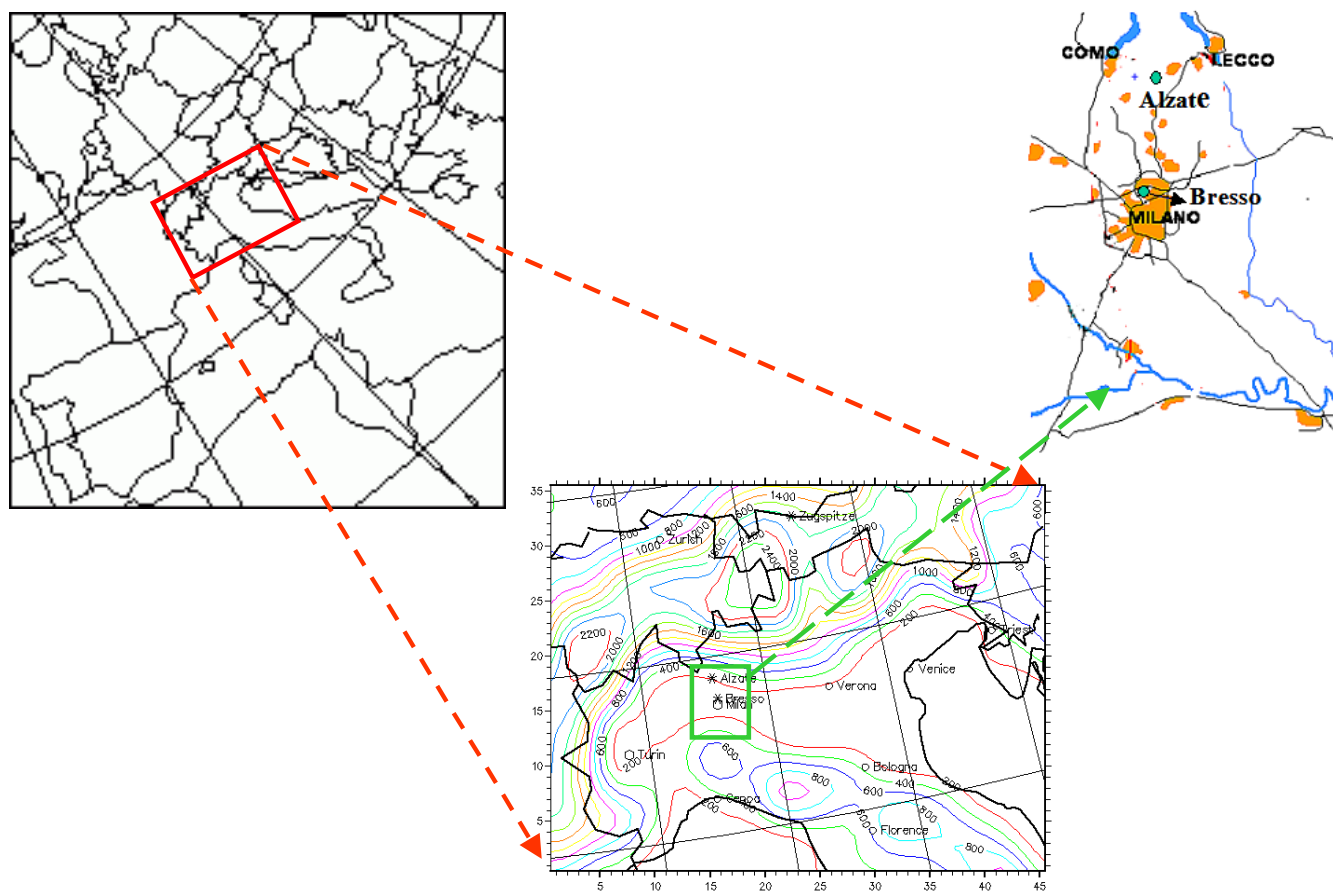


**Fig. 1.** The model domains for 50 km and 15 km resolutions, and campaign area in Po Basin. The position of the 15 km fine domain nested in the 50 km domain is outlined with a red rectangle. Ground based sites were located in the north of Milan, Bresso (urban site) and Alzate (semi-rural site).

of Milan and up to 30 km east of Milan. There were also two days where the flights were performed about 50 km to the south of Milan (13 and 15 August). Each aircraft mission lasted around three hours. The flight height followed the airspace regulations: it was about 600 m a.s.l. in the plain and up to 2700 m a.s.l. in the Alpine foothills. The aircraft measurements focused on HCHO, O<sub>3</sub> and aerosols. Meteorological parameters were recorded along the flight routes. Onboard the ultralight aircraft, formaldehyde was measured with a Hantzsch instrument (Kelly and Fortune, 1994). The detection limit for HCHO is ~50 ppt with a delay time of 90 s, and, assuming a flight velocity of 20 m/s, the horizontal resolution is about 2 km. The other instruments on the ultralight aircraft are described in detail by Junkermann et al. (2006).

## 2.2 Instrumentation and species

One of the most important objectives of the FORMAT project was to compare and improve the different measurement techniques used for measuring formaldehyde in the atmosphere.

Therefore, HCHO was intensively observed with various existing measurement techniques during the 2002 FORMAT campaign. The DNPH-HPLC method (Lee and Zhou, 1993) has been the main technique for the detection of formaldehyde, but new instruments with better time resolution and improved detection limits are now available. Among those, spectroscopic techniques like DOAS (Differential Optical Absorption Spectroscopy) (Cárdenas et al., 2000), TDLAS (Tunable Diode Laser Absorption Spectroscopy) (Fried et al., 1997), and FTIR (Fourier Transform Infrared Spectroscopy) (Lawson et al., 1990), and a fast in-situ Hantzsch technique using liquid phase fluorimetric detection have been widely used.

During the campaign period, five Hantzsch instruments were operated by three institutes for in-situ measurements of HCHO. Both the FTIR technique and the DOAS technique were used with White systems (White, 1976) for quasi in-situ measurements. The instruments and techniques were described by Hak et al. (2005). At the same time, a Long Path DOAS (LP-DOAS) was used for remote sensing at Alzate. With the purpose of understanding the ozone photooxidation

**Table 1.** Ground based measurement techniques and measured parameters during the 2002 FORMAT campaign.

Instrument type	Sampling	Sites	Componenets
DOAS Long Path	Long Path	Alzate	HCHO, O <sub>3</sub> , NO <sub>2</sub> , HONO, SO <sub>2</sub>
Enviro-nics 300 UV absorption	In-situ	Alzate	O <sub>3</sub>
Hantzsch	In-situ	Bresso & Alzate	HCHO
DOAS White-cell	In-situ	Bresso	HCHO, O <sub>3</sub> , NO <sub>2</sub> , HONO, SO <sub>2</sub>
FTIR White-cell	In-situ	Bresso	CO, HCHO
DNP	In-situ	Bresso&Alzate	HCHO
CO analyser AL5002 (Vacuum ultraviolet fluorescence)	In-situ	Alzate	CO
Thermoenvironment 42c (Ozone chemiluminescence)	In-situ	Alzate	NO
NO <sub>x</sub> TO <sub>y</sub> instrument (luminol chemiluminescence + NO <sub>y</sub> converter)	In-situ	Alzate	NO <sub>2</sub> , NO <sub>z</sub> , NO <sub>y</sub> , PANs, total nitrate
Meteo. station		Bresso/Alzate	T, P, relative humidity, wind direction and speed, global radiation

processes, additional species, such as O<sub>3</sub>, CO, NO, NO<sub>2</sub>, NO<sub>y</sub> (NO+NO<sub>2</sub>+NO<sub>3</sub>+N<sub>2</sub>O<sub>5</sub>+PAN+HNO<sub>3</sub>+HONO), HNO<sub>3</sub>, and PAN were measured. Table 1 gives a description of the instruments used and species measured during the 2002 campaign. Meteorological stations were operational at both sites.

### 2.3 Meteorological conditions

The meteorological conditions during the 2002 campaign period were characterized by more unstable weather than usual. Temperatures were lower, and there was more precipitation than usual. During the FORMAT campaign, three fair weather periods were identified. The first period was from 22 to 31 July. This period was dominated by a high-pressure system, and high radiation during daylight hours (average above 350 W/m<sup>2</sup> between 08:00–20:00 LT). Temperatures exceeded 30°C only on 31 July. After a few unstable days with short shower events, 7–8 August again showed fair weather conditions with high radiation and moderately high temperatures. During the period from 9 to 12 August, a low-pressure system associated with precipitation passed over the area. The last days of the campaign, from 13 to 20 August, were again dominated by a high-pressure system, leading to stable weather, and favourable conditions for photochemical reactions. Six flights were carried out during the last fair weather days, and an intensive observation period (IOP) was held during this period.

The wind patterns during summer in the Po Basin are strongly controlled by thermodynamic circulation. Due to the presence of the Alpine foothills in the north, the dominating winds are northerly during nighttime, and southerly during the day. As a consequence, ozone peaks are often found in the afternoon downwind of Milan, in the north of the Po Basin. Several studies for this area have shown the

wind evolution and observed high ozone levels north of Milan during the summer months (Prévôt et al., 1997; Martilli et al., 2002; Thielmann et al., 2002; Baertsch-Ritter et al., 2003, 2004; Andreani-Aksoyoglu et al., 2004). During the 2002 campaign, the meteorological stations at Alzate and Bresso showed similar wind patterns as in other years. Winds blew from the north during the night and early morning, turned to southerly before noon, and changed to northerly in the evening again. The turning time of the wind direction is important for the transport of the Milan plume.

Three North Foehn days (7, 12 and 13 August) were identified during the campaign period according to the criteria described by Forrer et al. (2000). The North Foehn brings air masses from the free troposphere above the Alpine crest to the boundary layer, and is characterized by strong winds and low relative humidity. Meanwhile, differences in pressure and potential temperature are small between stations in the Po Basin and the high-altitude stations in the Alps. During North Foehn events, the air quality south of the Alps and in the highly polluted Po Basin is clearly improved compared to other days. The frequency of North Foehn days is about 4–6% during the summer months (Weber and Prévôt, 2002). Meteorological data from Jungfraujoch (3600 m a.s.l.) and Alzate (404 m a.s.l.) were used to identify the North Foehn days. Figure 2 shows the time series of pressure, temperature, radiation, relative humidity, wind direction and wind speed at Alzate during this period. The three North Foehn days are marked by dashed lines.

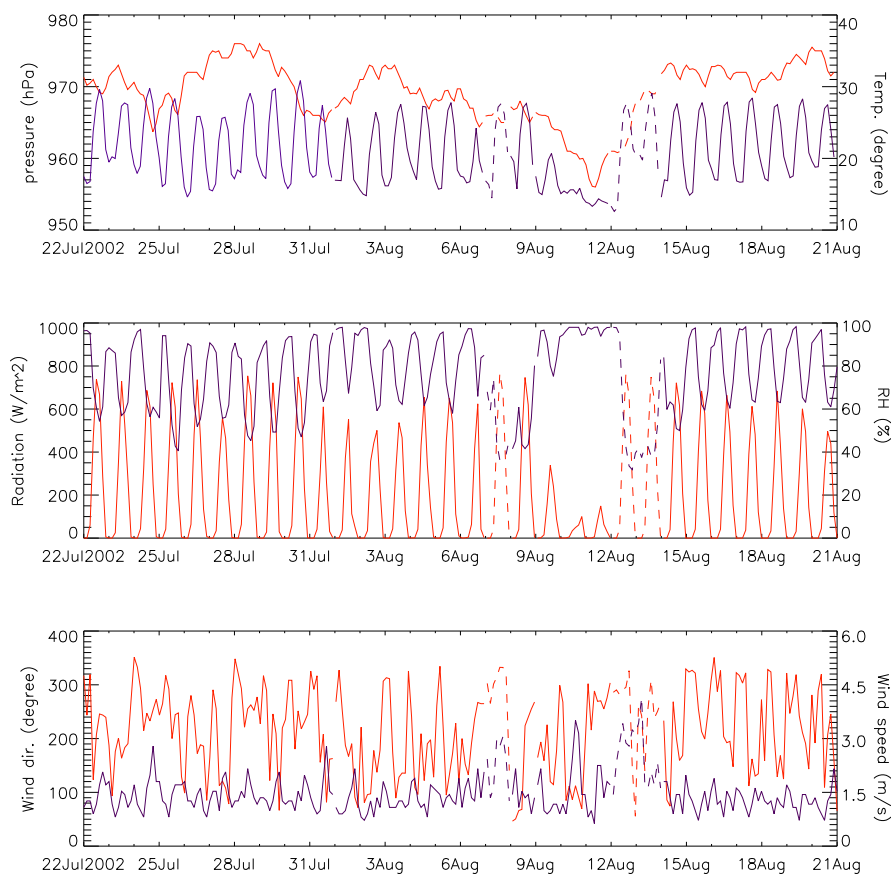


**Fig. 2.** Meteorological conditions measured at Alzate during the campaign period. The north Foehn days are marked by dashed lines, the episodes are characterized with high wind speed and low relative humidity. 1st panel: pressure (red) and temperature (blue); 2nd panel: global radiation (red) and relative humidity (blue); 3rd panel: wind direction (red) and wind speed (blue).

### 3 Model description

#### 3.1 Model description

The NILU regional chemical transport model (RCTM) is driven by meteorological data from a Numerical Weather Prediction (NWP) model, which is based on the NORLAM model from the Norwegian Meteorological Institute (Grønås et al., 1987; Nordeng, 1986). Global meteorological analyses and forecasts from ECMWF (European Centre for Medium Range Weather Forecasts) are used as initial and boundary conditions. The model uses sigma coordinates and stereographic map projection. Horizontal resolutions of the model can be defined from 150 to 15 km at 60° N. The model uses one way nesting and provides the coarse scale chemistry output as boundary conditions for the fine scale model. A detailed description of the chemistry transport model can be found in Flatøy and Hov (1996).

In the transport part of the CTM, a second-order version of the advection scheme by Bott (1989) is used, and the semi-Crank-Nicholson scheme is used for diffusion. The vertical

transport occurring in convection is calculated with a modified version of the asymmetrical convection model (ACM) proposed by Plum and Chang (1992). Parameterization of the vertical transport of chemical tracers in connection with convective plumes and the compensating sinking motion was introduced by Flatøy and Hov (1995). Dry deposition rates are computed as a function of latitude, time of day, time of year, land type, vegetation type, and meteorological conditions according to McKeen et al. (1991) and Hass (1991). The wet deposition is calculated based on the rate of precipitation at the ground, on the rainout rate from the individual vertical layers, and on the wet scavenging coefficients for individual species. For more details about dry and wet deposition see Hov et al. (1988), Strand and Hov (1994) and Flatøy and Hov (1995).

The chemistry scheme in the NILU RCTM includes a comprehensive description of gas phase chemistry with particular emphasis on photochemical oxidants. The chemistry scheme is documented by Flatøy and Hov (1995, 1996). The chemistry is rather similar to the one used in the global two-dimensional model by Strand and Hov (1994) to study global

tropospheric ozone. A lumped chemistry scheme is used in the model. The chemical description includes about 110 reactions involving 55 species in the gas phase, aerosol loss is parameterized.

Surface emissions are specified for  $\text{NO}_x$ , CO, VOC and  $\text{SO}_2$ . In this study, the emissions from CITY-DELTA (<http://aqm.jrc.it/citydelta/>) for the Milan region were employed for the 15 km grid, emissions from EMEP for 2002 (Berge, 1997) were used on the 50 km grid and on the 150 km domain data from EDGAR (Van Aardenne et al., 2001) for 1995 were used. Emissions were employed with monthly/weekly/hourly variation factors. Natural VOC emissions, as a major source of biogenically produced HCHO, were represented by isoprene in the model. The model calculates the isoprene emission from data on forest cover (land use and forest type) and surface temperature, using a method from Lübker and Schöpp (1989).

### 3.2 Model set up

In this study, the nested model was defined with the horizontal resolutions of 150, 50 and 15 km, 10, 18 and 30 unequally spaced vertical levels were used, respectively, with a model top defined at 100 hPa. Figure 1 shows the model domains with resolution of 50 km and 15 km. Meteorological analysis from ECWMF are used as initial and boundary conditions for NWP prognoses on the three domains, and the meteorological forecasts are stored with one-hour resolution. The 150 km resolution grid covers most of the Northern Hemisphere, and initial and boundary values for all components are fixed to values that are representative for an unpolluted atmosphere. The 50 and 15 km models receive boundary input from the 150 and 50 km grids, respectively. Model results were stored with 3-h resolution for comparison with surface measurements during the whole campaign period. For the days with aircraft observations, model results were stored with one-hour resolution.

## 4 Results and discussion

### 4.1 Comparison of model results and measurements of HCHO

#### 4.1.1 Bresso

From 23 to 31 July, the ground-based in-situ instruments for HCHO measurements were operated at Bresso for intercomparison. In order to compare with the in-situ instruments, both DOAS and FTIR measurements were carried out with White systems. Five Hantzsch instruments run by three participants analyzed the air from a common inlet line. Figure 3a gives a diagram of the instrument setup at Bresso. The use of the White systems for the optical techniques excluded spatial gradients of HCHO as potential error sources, and ensured the sampling of nearly the same air masses by

all instruments. The instrument intercomparison experiment concluded that the agreement between different techniques or similar techniques for HCHO measurements of the same air mass was good. The detailed discussion about equipment setup and data analysis was described and discussed by Hak et al. (2005).

The model results for HCHO at Bresso show fairly good agreement with the measurements, but there are some peaks in the measurements that are not captured by the model (second panel of Fig. 4). However the bulk part of the modelled and measured concentrations are in the same range of 2–6 ppb. This site is exposed to emissions from the city when the winds are from the south, and emissions from the industrial area in the northern part of Milan, when the wind blows from the north. Some HCHO peaks that are not reproduced by the model are possibly caused by primary emissions in the immediate vicinity of the measurement site.

#### 4.1.2 Alzate

In this section, we will focus on the results from Alzate, where both remote sensing (long path DOAS) and in-situ (Hantzsch) instruments were deployed. Figure 3b gives a scheme of the instrument setup at Alzate. The site is close to a small airfield, on the edge of a maize field. The Hantzsch instrument was inside a container, with an inlet about 2.5 m above the ground. The LP-DOAS telescope was inside another container, and the retro-reflector array to reflect the light beam was 2190 m away and 35 m above the ground on a telecommunication tower. The light path of the LP-DOAS crossed the maize field and grassland in the first 200 m, and beyond them there was dense forest underneath. Because of the vegetation and anthropogenic activities, high concentrations and variability might be possible at Alzate as well. The HCHO measurements from both instruments agree well during most days when the radiation was low. On days with high radiation, there were significant differences between HCHO measurements by the Hantzsch instrument and long path DOAS as it will be discussed in the next paragraph. On some days the LP-DOAS measured twice as much HCHO as the Hantzsch instrument.

The model results agree well with the Hantzsch measurements for the fair weather days with the few exception on 26, 29, 30, 31 July. (see Fig. 4 and discussion of Fig. 6). On 11 August there were rain showers measured that could not be captured by the model leading to a significant overestimation of HCHO on that day. We will consider only the fair weather days for the further discussion. The median values between 12 h and 17 h of the three datasets were calculated for fair weather periods: 1.95 ppb for Hantzsch, 3.60 ppb for LP-DOAS, and 2.06 ppb for model results, respectively. The median levels between 08:00 h and 11:00 h during the same period were 1.22 ppb for Hantzsch, 2.03 ppb for LP-DOAS, and 1.57 ppb for model results. The high levels of HCHO observed by the LP-DOAS are most probably caused by

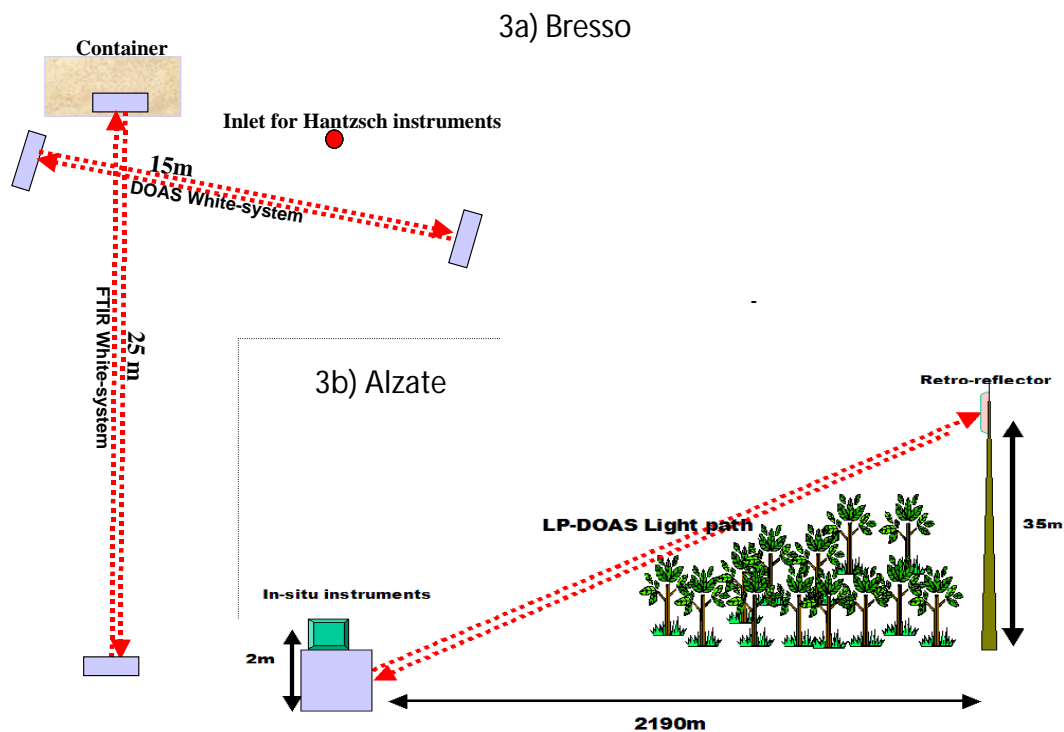


**Fig. 3.** Instruments set up at two surface stations. (a) Ground based instruments set up at Bresso (in-situ instruments only); (b) Instruments set up at Alzate (both in-situ and remote sensing instruments).

biogenic emissions, because the light path of the LP-DOAS mostly passes over a forest where HCHO is formed from isoprene emitted underneath. Isoprene is a reactive hydrocarbon that is released mainly by deciduous forests, particularly on days with high temperature and radiation. The isoprene levels reach about 1 ppb between 12:00 h and 17:00 h in Alzate, and evening peaks up to 3 ppb were measured during the IOP (Steinbacher et al., 2005). Those measurements were made close to the container, about 200 m away from the forest, so the isoprene levels above the forest in the afternoon hours could be much higher. The isoprene emissions estimated by Steinbacher et al. (2005) show that the highest levels are expected during the afternoon hours. The modelled HCHO concentrations are between the Hantzsch and LP-DOAS measurements and this is expected, since the area of the isoprene-emitting forest is averaged over the whole grid cell. This explains why the model provides less formaldehyde than the LP-DOAS, whose light beam passed directly over a forest area, and also why the model calculates more HCHO than the in-situ measurements, which are hardly influenced by isoprene emitting trees.

A scatter plot for HCHO at Alzate is shown in Fig. 5 (right panel). The afternoon data from the good weather period were used, and the model results were compared to both Hantzsch and LP-DOAS measurements. The data points between model results and Hantzsch measurements mostly

fall within the 1:2 and 2:1 lines. The standard deviation is 0.39 for model results and 0.46 for Hantzsch measurements, which shows that the model captures the HCHO levels fairly well. The average difference between modelled and in-situ measurements (Hantzsch) is small, about 0.09 ppb, although the correlation is low (0.42), since the model simulated peaks occur at an earlier time than the measured ones. Also the small variations of model results lead to a rather low correlation coefficient in spite of the good absolute concentration agreement. The model output was given every three hours, whereas the instrument recordings have a much higher time resolution. Therefore, some measured peaks may not be included in the model time series. Another reason is the difference between simulated and real wind direction. The last few days of the campaign period, simulated and real wind directions generally agree well, but the simulated winds are generally more monotonic, compared to the real wind direction. Because HCHO has a lifetime of a few hours and O<sub>3</sub> of a few days, these factors can have a higher impact on HCHO than on the O<sub>3</sub> concentration. The average difference between measured HCHO from the remote sensing instrument (LP-DOAS) and model results is 1.55 ppb, with a correlation of 0.58. The modelled levels are between those of in-situ and remote measurements, and more close to the in-situ measurements. Because of the short lifetime of HCHO and its diverse sources, it can easily be influenced by transported

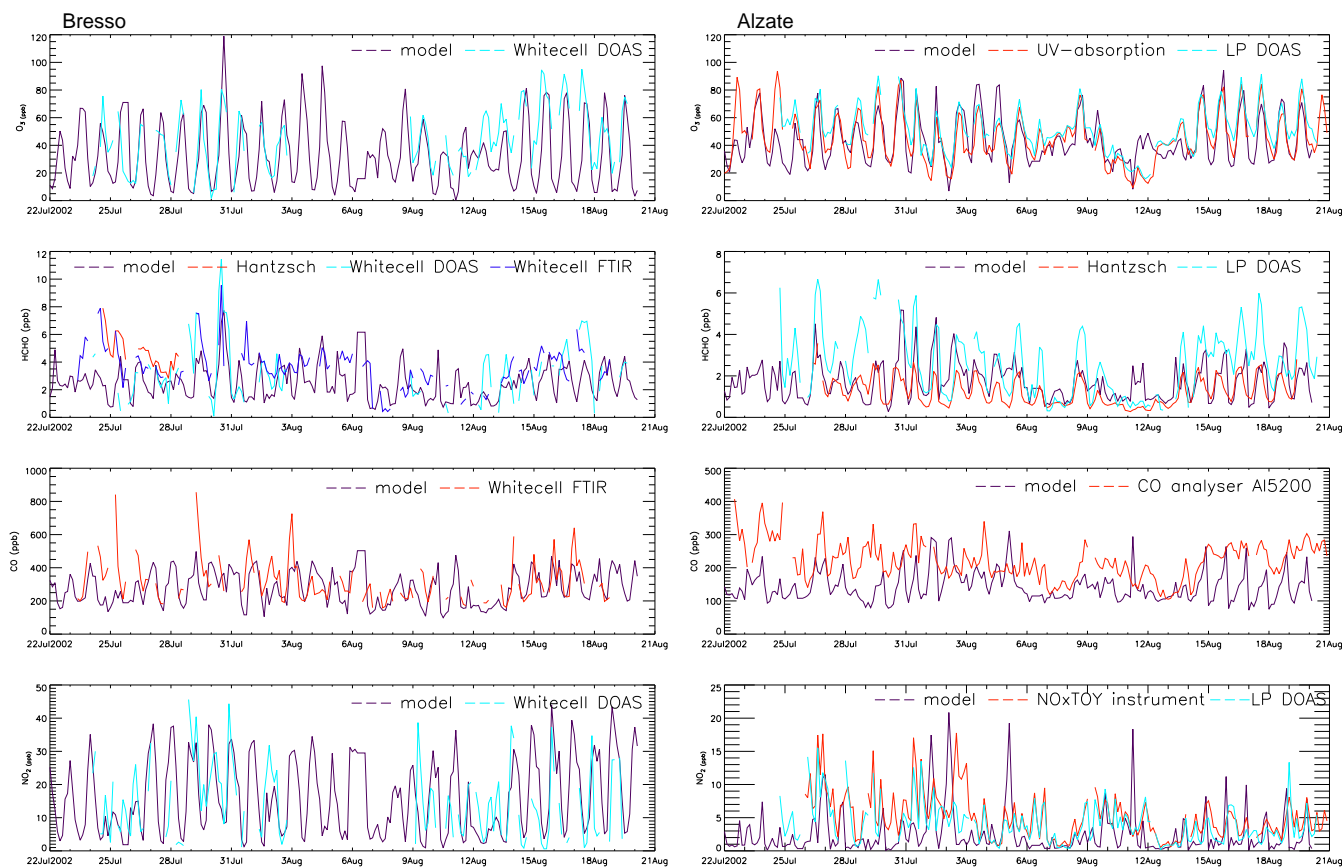


**Fig. 4.** Modeled and measured mixing ratios of  $O_3$ , HCHO, CO,  $NO_2$  every 3 h (LT) at Bresso and Alzate during the campaign period.

air masses and small scale fluctuations, whereas the model results are representing the average situation over  $125 \text{ km}^2$ . The data points in the model against LP-DOAS plot are often outside the 1:2 and 2:1 lines, and the standard deviation is high (1.34 ppb). As explained earlier, these high values are likely caused by local biogenic emissions from the nearby forest. These results show that the instrument setup is crucial in order to obtain HCHO measurements that are representative for a larger area, such as a model grid cell of  $15 \times 15 \text{ km}^2$ . This argument will also apply to other short-lived species that are emitted by or rapidly formed from local sources.

The main source of secondary HCHO is the oxidation of VOCs by reaction with the OH radical. As a consequence, the production of HCHO can be considered proportional to the VOCs and the OH radical content of the air (Reaction R1). The photolysis of ozone to form excited atomic oxygen  $O(^1D)$  and the subsequent reaction between  $O(^1D)$  and water are usually the major source of OH in the afternoon for clean air. Therefore, production of [OH] can be approximated by reaction (Reaction R2). Considering the loss of HCHO, photolysis of HCHO is a major loss process during the day with clear sky. Both  $J(\text{HCHO})$  and  $J(O(^1D))$  are proportional to the incoming actinic flux. Since radiation

contributes both to HCHO production and loss, we might disregard the photolysis terms and investigate the relationship between HCHO and  $(R_{\text{VOC}} \times O_3 \times H_2O)$  by combining the Reactions (R1) and (R2). If two different instruments, such as Hantzsch and LP-DOAS, give different HCHO amounts for the same value of  $(O_3 \times H_2O)$ , this most probably means that the different air masses probed by the two measurements must contain different amounts of reactivity weighted VOCs. We will in the following use scatter plots of HCHO vs.  $(O_3 \times H_2O)$  to further compare model results and measurements.

$$P(\text{HCHO}) \propto \sum_{i=1}^N k_i \times [\text{VOC}_i] \times [\text{OH}] \equiv R_{\text{VOC}} \times [\text{OH}] \quad (\text{R1})$$

Where  $R_{\text{VOC}}$  is reactivity weighted VOC

$$P(\text{OH}) \cong [O_3] \times [H_2O] \times J(O(^1D)) \quad (\text{R2})$$

Figure 6 shows scatter plots of HCHO vs.  $(O_3 \times H_2O)$  from model results and from measurements with Hantzsch and LP-DOAS. Only data from afternoon hours (11:00–17:00 LT) on fair weather days were used. The slopes of the regressions in Fig. 6 are 1.67, 1.96 and 4.65 for model, Hantzsch and



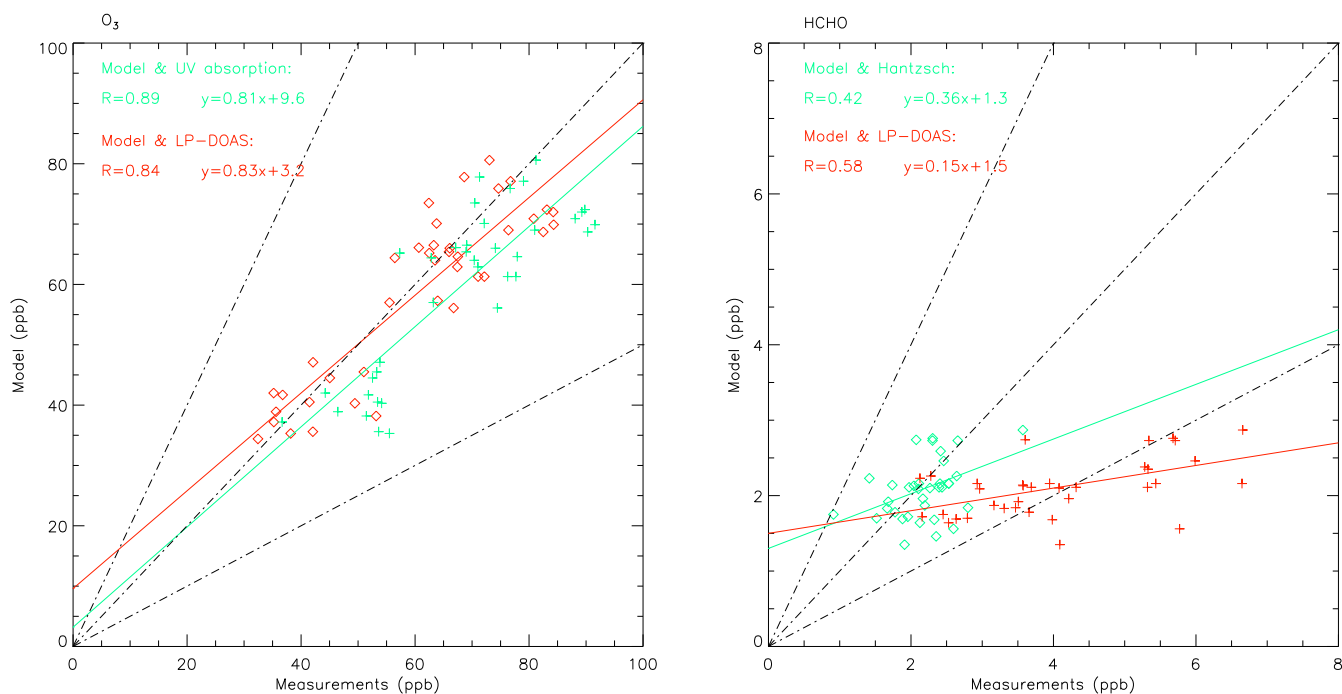
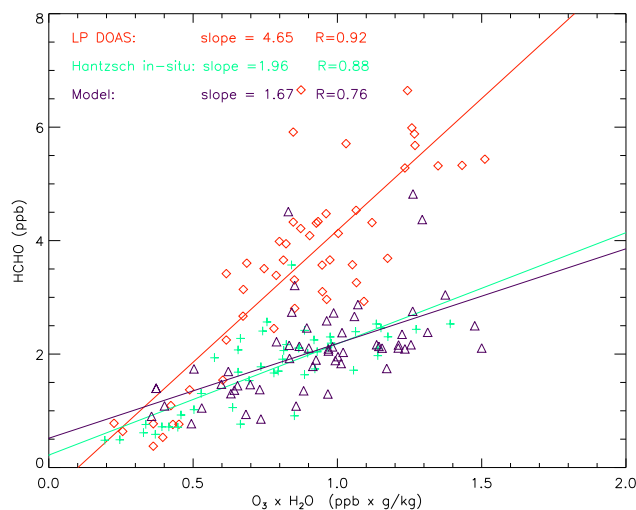


**Fig. 5.** Scatter plots of modelled and measured  $O_3$  and HCHO at Alzate. Only afternoon data from fair weather days are used. Solid lines represent the regression lines, and dotted lines represent the 1:2, 1:1, and 2:1 lines.

LP-DOAS, respectively. As expected, the model agrees better with the in-situ Hantzsch than with the remote sensing LP-DOAS. This indicates that model and in-situ data represent air masses with similar VOC chemistry. Results from the remote sensing instrument (LP-DOAS), show that the instrument sampled different air masses with very high HCHO levels. The LP-DOAS measurements are influenced by local biogenic emissions, which are not seen as average conditions in the model's grid cell. Because the model does not contain primary HCHO emissions, this comparison is based on the assumption that all HCHO at this site are secondary produced. This is reasonable since there are no significant direct emissions of HCHO around Alzate, and also the lifetime of HCHO is short compared to the advection time. The agreement between the model and the Hantzsch measurements shows that the model is able to reproduce the formaldehyde mixing ratios in a satisfactory way. It is important to keep in mind, when comparing model results and measurements, that the instrument setup and type have to be taken into account.

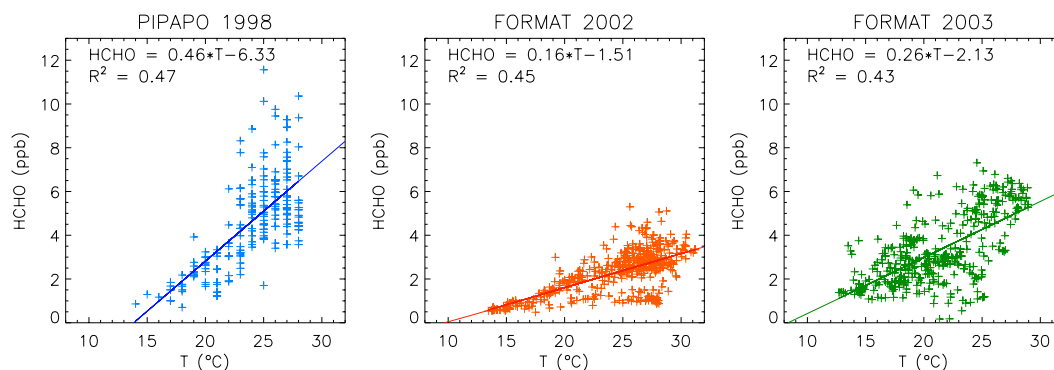
#### 4.2 Concentrations and temporal variations at Bresso and Alzate

Figure 4 shows the temporal variation of model results close to the surface and measured concentrations of  $O_3$ , HCHO, CO and  $NO_2$  at Bresso (left panel) and Alzate (right panel) with 3 h resolution between 22 July and 20 August.



**Fig. 6.** Scatter plot of HCHO vs. ( $O_3 \times$  specific humidity) for model results and measurements from both in-situ and remote sensing instruments at Alzate. Only afternoon data from fair weather days are used.  $O_3$  and HCHO are in ppb, and water content is g/kg.

During the campaign period, the highest daily surface ozone maximum was around 90 ppb. Compared with the measurements from PIPAPO in May–June 1998 (the highest level was 190 ppb) and the levels in September–October 2003 FORMAT campaign (the highest level was 135 ppb) at the same location, the concentration is unexpectedly low for



**Fig. 7.** Regression of the afternoon ozone concentrations against temperature for three field campaigns: PIPAP0 1998 (May–June), FORMAT 2002 (July–August), and FORMAT 2003 (September–October).

this time of the year. These relatively low maximum levels can be explained by unstable weather conditions in this period, or by the low emissions during the Italian summer vacation in August. According to the emissions inventory from CITY DELTA, both CO and VOC emissions decrease by about 15% because of the lower industrial activity during the summer vacation. NO<sub>x</sub> emissions are only 5% lower, because the reduced work related traffic was compensated by increased tourist traffic during this period.

Afternoon O<sub>3</sub> levels are usually correlated with temperature in summer (e.g. Neftel et al., 2002; Weber and Prévôt, 2002; Ordóñez et al., 2005). Figure 7 shows the regression of the afternoon ozone mixing ratios against temperature for three campaigns: PIPAP0 1998, FORMAT 2002, and FORMAT 2003. The slope of the linear regression between O<sub>3</sub> concentration and temperature was rather small for the FORMAT 2002 campaign in comparison to the PIPAP0 and FORMAT 2003 campaign. Both the temperature itself and the other meteorological factors represented by temperature, such as radiation, cloud cover and humidity, affect the photochemical processes (e.g. decomposition of PAN, emission rate of biogenic VOCs, photolysis rates, etc.). The low slope of the ozone vs. temperature regression found in the 2002 campaign shows the influence of unstable weather conditions, and also the effect of the summer vacation on O<sub>3</sub>.

Both at Alzate and Bresso, measured and modelled ozone show a typical pattern for the summer time, with low mixing ratios in the night and peaks during the late afternoon. The left panel of Fig. 4 depicts the time series for Bresso, the site most influenced by local emissions. Observed ozone levels during the campaign period for Bresso ranged from a few ppb up to 95 ppb. The low ozone levels during nighttime are mainly caused by titration with NO, due to local emissions from the city. Modelled ozone at Bresso is in good agreement with observations both in the magnitude of the O<sub>3</sub> concentrations and the diurnal variation. Measured HCHO, CO and NO<sub>2</sub> show strong influence from local emissions, and some peaks can be ascribed to local sources. There were

a few days within the last fair weather period when the modelled ozone was lower than measured during nighttime, and the modelled NO<sub>2</sub> was higher than the measurements. This can be explained by a too low mixing height in the model, trapping emissions during the night and causing significant ozone loss from dry deposition and ozone loss by reaction with NO. At Alzate (Fig. 4, right panel), ozone levels and time variation simulated by the model generally agree well with measurements. Figure 5 shows a scatter plot of modelled and measured O<sub>3</sub> at Alzate (left panel). The afternoon data from the good weather period were used, and the model results were compared with both in-situ (UV absorption) and remote sensing measurements (LP-DOAS). The regression analysis shows that model simulated O<sub>3</sub> agrees well with both the in-situ and remote sensing measurements. A high correlation value (0.89 and 0.84) and a slope close to 1 (0.81 and 0.83) are found between measured and modelled O<sub>3</sub>. A small average difference of 1.9 ppb is found between model results and in-situ measurements, and the average difference between LP-DOAS and model results is about 9.1 ppb. The standard deviations for the three data sets are of similar magnitude with values of 14.3 for model results, 15.6 for in-situ measurements, and 14.4 for LP-DOAS. All the data points fall well within the 1:2 and 2:1 lines. Although the model reproduces the ozone concentrations well during daytime, it underestimates the ozone levels during nighttime, especially during nights with clear sky. In the same way as in Bresso, this might be due to an overestimated influence of dry deposition close to the surface during nighttime. Since 18 August was a Sunday, the drop of O<sub>3</sub>, CO and NO<sub>2</sub> was possibly due to the weekend effect. On 11 August, which was the day with precipitation, the model calculated much higher levels for ozone and HCHO than the observations. That day the NWP model didn't produce any rainfall, and the temperatures were overestimated as well. This explains the discrepancy.

Both CO and NO<sub>x</sub> have a large number of sources in the Po Basin. The median CO concentration at Bresso is only

about 285 ppb, following the reduced emissions during this period. The results from Bresso indicate that the model is able to provide good estimates of both CO and NO<sub>2</sub> mixing ratios. The simulated concentrations of CO and NO<sub>2</sub> are generally underestimated at Alzate, mainly due to the averaged emissions in the model grid cells. The results from Alzate show that the thermally induced circulation was more clearly identified by the model, that clean air arrived from the mountains in the night, and that polluted air arrived from the south in the early or late afternoon. The modelled evening peaks of CO and NO<sub>2</sub> at Alzate suggested that the model was able to capture the afternoon arrival of the plume from the south, but the modelled transport from the north in the morning was too strong.

North Foehn events were identified on 7, 12 and 13 August, where strong winds from the Alpine crest brought dry and clean air from the free troposphere. On 13 August, the meteorological data showed weaker Foehn character than on the other two days. Despite high temperature and radiation, the observed ozone levels remained below 60 ppb both at Alzate and Bresso during these days. Such mixing ratios are representative of high altitude air above the Alps (Weber and Prévôt, 2002). Also the CO and NO<sub>2</sub> observations showed low mixing ratios: CO was about 200 ppb at Bresso and 100 ppb at Alzate. The model is in good agreement with measurements during the identified North Foehn days.

#### 4.3 Slopes of O<sub>3</sub> versus NO<sub>z</sub> at Alzate

During the campaign, the last identified fair weather period, i.e. IOP (13–20 August) had the most stable weather conditions. For several days, the ground O<sub>3</sub> levels measured at Alzate were around 90 ppb, and the highest O<sub>3</sub> level (127 ppb) was measured in an area southwest of Alzate at 14:00 h on 17 August by the aircraft. Except the North Foehn day (13 August), the weather conditions were similar for all these days. Overall the northerly winds came from the Alps during the night and changed to southerly from about 08:00–09:00 LT until 20:00 LT. During the campaign the south-southeasterly winds were dominating during daytime, and the wind speeds were ~1.5 m/s. This means that air masses from the edge of Milan metropolitan area needed 3–4 h to reach Alzate. For ozone production sensitivity studies, ozone production efficiency is important. In some cases, the slope of O<sub>3</sub> versus NO<sub>z</sub> ( $\Delta\text{O}_3/\Delta\text{NO}_z$ ) can be interpreted as the ozone production efficiency, i.e. as the number of O<sub>3</sub> molecules produced for each NO<sub>x</sub> consumed, where NO<sub>z</sub> (NO<sub>y</sub>-NO<sub>x</sub>) represents consumption of NO<sub>x</sub> (Lin et al., 1988; Trainer et al., 1993). Thielmann et al. (2002) studied several cases at Alzate by analyzing the measurements, and concluded that the ozone production in the Milan plume is strongly controlled by VOCs. They found that  $\Delta\text{O}_3/\Delta\text{NO}_z$  was about 2.2, and the ozone background level was 93.1 ppb during the afternoon hours (15:00–17:00 LT) in May 1998. Prévôt et al. (1997) performed aircraft measurements over

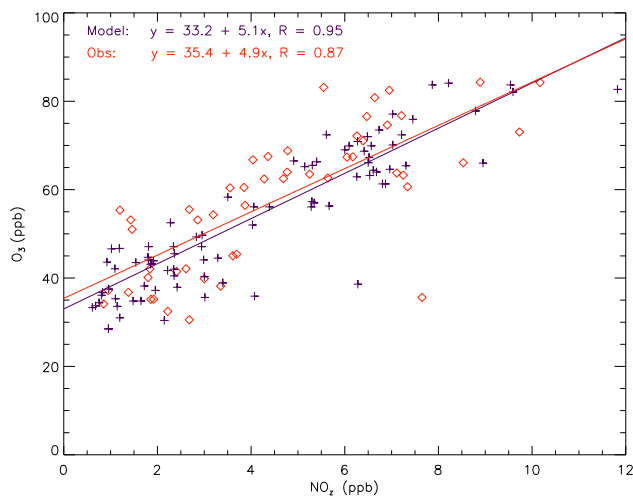
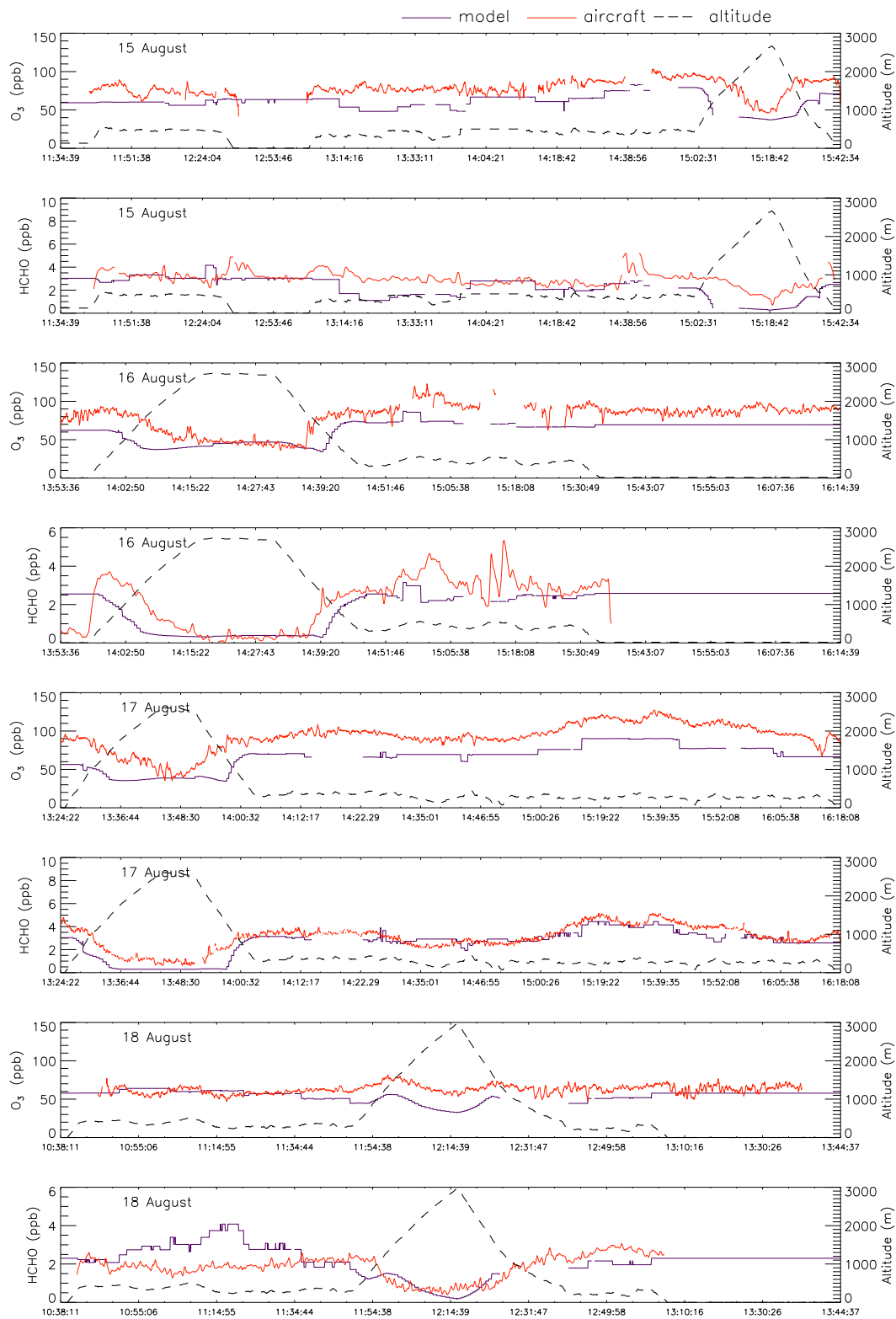


**Fig. 8.** Scatter plot of both modeled and measured O<sub>3</sub> and NO<sub>z</sub> at Alzate during the fair weather period. Both measurements (UV absorption) and model results were 3-h resolution.

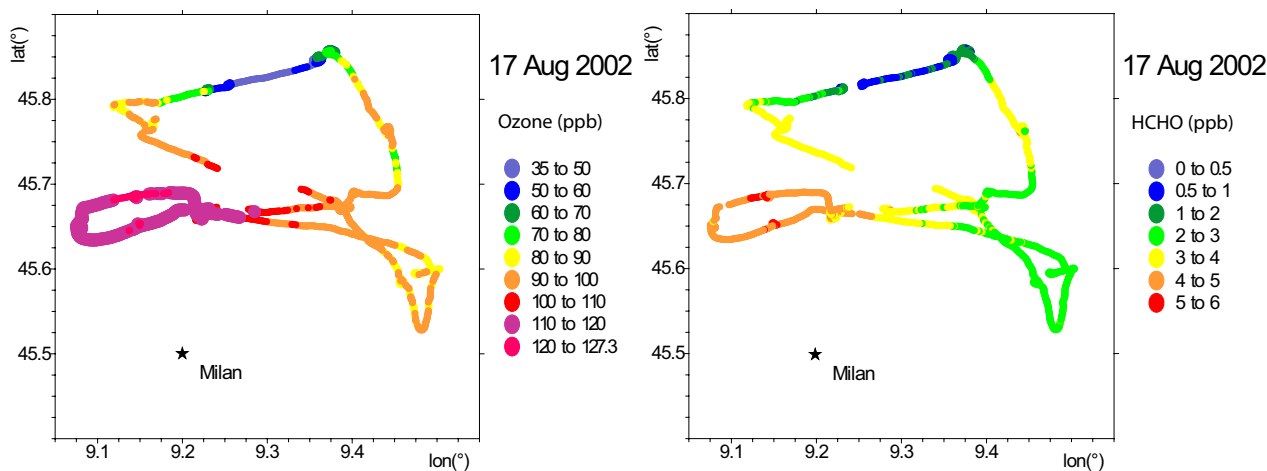
the Southern Alps in July 1993. A  $\Delta\text{O}_3/\Delta\text{NO}_z$  value of 4.2 was found for the flight route in the vicinity of Alzate, whereas  $\Delta\text{O}_3/\Delta\text{NO}_z$  was 13.6 for the more rural areas.

Figure 8 illustrates both modeled and measured scatter plots of O<sub>3</sub> vs. NO<sub>z</sub> at Alzate. In the figure, both measurements and model results are averaged between 12 h and 17 h. The slope of O<sub>3</sub> vs. NO<sub>z</sub> is 4.9 for the measurements and 5.1 for the model. This value is higher than the value 2.2 calculated by Thielmann et al. (2002), who found that Alzate was strongly influenced by the Milan plume. Our results are very similar to the value presented by Prévôt et al. (1997), where the aircraft flew over a large area influenced by the regional plume. The differences can be explained by the location and strength of the plume due to less emissions by the vacation effect. Since the dominating winds come from the southeast, Alzate might be located on the edge of the plume, and hence not so strongly influenced by the urban plume. This is supported by the measurements of NO<sub>z</sub> and nitrates (not shown) at Alzate, that both peaked at the same time as O<sub>3</sub>, although the levels were low. The decreased emissions due to the vacation effect can be another reason for lower O<sub>3</sub> production in this period, since the ozone production obviously depend on the levels of precursors (Liu et al., 1987; Lin et al., 1988).

Similar O<sub>3</sub> background levels during the afternoon hours have been calculated from both data sets: 33 ppb for model and 35 ppb for measurements (see the intercepts in Fig. 8). These levels are much lower than those in Thielmann et al. (2002) and Prévôt et al. (1997). They reported 93.1 ppb for the afternoon hours in May 1998 at Alzate, and 79.4 ppb for the areas in the vicinity of Alzate in July 1993, respectively. The background levels of O<sub>3</sub> during the afternoon hours represent the levels in the well-mixed boundary layer. They give information on emissions and the ozone build up



**Fig. 9.** Simulated (violet) and measured (red) HCHO and  $O_3$  concentrations along the flight tracks (Local Time). The flight height is given by the dashed line.



**Fig. 10.** HCHO and  $O_3$  concentration measured during the flight on 17 August 2002. The colours of points show the ranges of the concentrations along the flight track. For ozone: dark blue: 35–50 ppb; blue: 50–60 ppb; dark green: 60–70 ppb; green: 70–80 ppb; yellow: 80–90; orange: 90–100 ppb; red: 100–110; purple: 110–120 ppb; rosy: 120–127.3 ppb. For HCHO: dark blue: 0–0.5 ppb; blue: 0.5–1 ppb; dark green: 1–2 ppb; green: 2–3 ppb; yellow: 3–4; orange: 4–5 ppb; red: 5–6.

based on the meteorological conditions. During the last fair weather period, the combined photochemical production and background levels produced  $O_3$  peak levels of about 90 ppb at Alzate. The low background levels during the campaign period are caused by lower emissions and unstable weather conditions probably also play an important role for the  $O_3$  peak levels.

#### 4.4 Comparison with aircraft measurements

The period from 13 to 20 August was characterized by stagnant conditions, which is favourable for ozone production and accumulation. A total of 6 flights (13, 14, 15, 16, 17 and 18, August) were performed during this period. Figure 9 shows modelled and measured  $O_3$  and HCHO along the flight tracks on 15, 16, 17 and 18 August. Data measured on 13 and 14 August were excluded, because of calibration problems on 13 August and because of shortage of data on the 14 August.

Because of the thermal winds from the south during daytime, both HCHO and  $O_3$  were expected to peak in areas north of Milan. On 15, 16 and 17 August, the ozone peaks were measured by aircraft at about 15:00 LT in this region. The peak values were 104 ppb on 15, 123 ppb on 16, and 127 ppb on 17 August. The meteorological conditions were similar for these three days. Since the flight on 15 August mainly took place over areas north, east and south of Milan, the flight track did not cross the Milan plume. However, the fact that both aircraft measured ozone and formaldehyde mixing ratios (104 and 5.22 ppb of maximum concentration, respectively) as well as the aerosol concentrations (not shown) were elevated and peaking at the same location shows that the measured air mass was influenced by the pol-

lution from the urban area of Milan. The flight on 18 August started earlier, finished at about 13:00 h and covered the area of the north and east of Milan. Southeast winds were dominating during this flight, and the highest ozone level measured was 82 ppb north of Milan at around 12:00 LT, too early to catch the Milan plume. The model results along the flight tracks show good agreement with the measurements. The comparison of mixing ratio levels and their temporal variation indicates that the model is able to reproduce the  $O_3$  and HCHO most of the time both for transport and photochemical processes in this area. Some HCHO peaks are not captured. These peaks are possibly caused by local primary emissions. Analysis of FORMAT data suggests that the HCHO in the northern part of the Po Basin is mainly photochemically produced (manuscript in preparation). Further modelling sensitivity studies including HCHO emissions (in these model runs, no HCHO emissions were used) would be useful.

Figure 10 shows the flight track followed by the aircraft on 17 August. The colour coding represents the mixing ratios of ozone (left hand panel) and HCHO (right hand panel). From this figure one can clearly see that the Milan plume was located northwest of the city. Both  $O_3$  and HCHO measurements distinguish the plume from the surroundings. Measured  $O_3$  levels were above 120 ppb inside the plume, and surrounding areas have ozone levels around 90 ppb. These very high concentrations were likely due to ozone concentration build-up during several days with fair weather conditions. The model ozone levels above 120 ppb (not shown) were found up to 700 m in a well-mixed HCHO peak was above 7 ppb close to the surface (Fig. 11), and about 6 ppb at flight altitude in the plume whereas the aircraft measurements reach somewhat lower maximum values of around

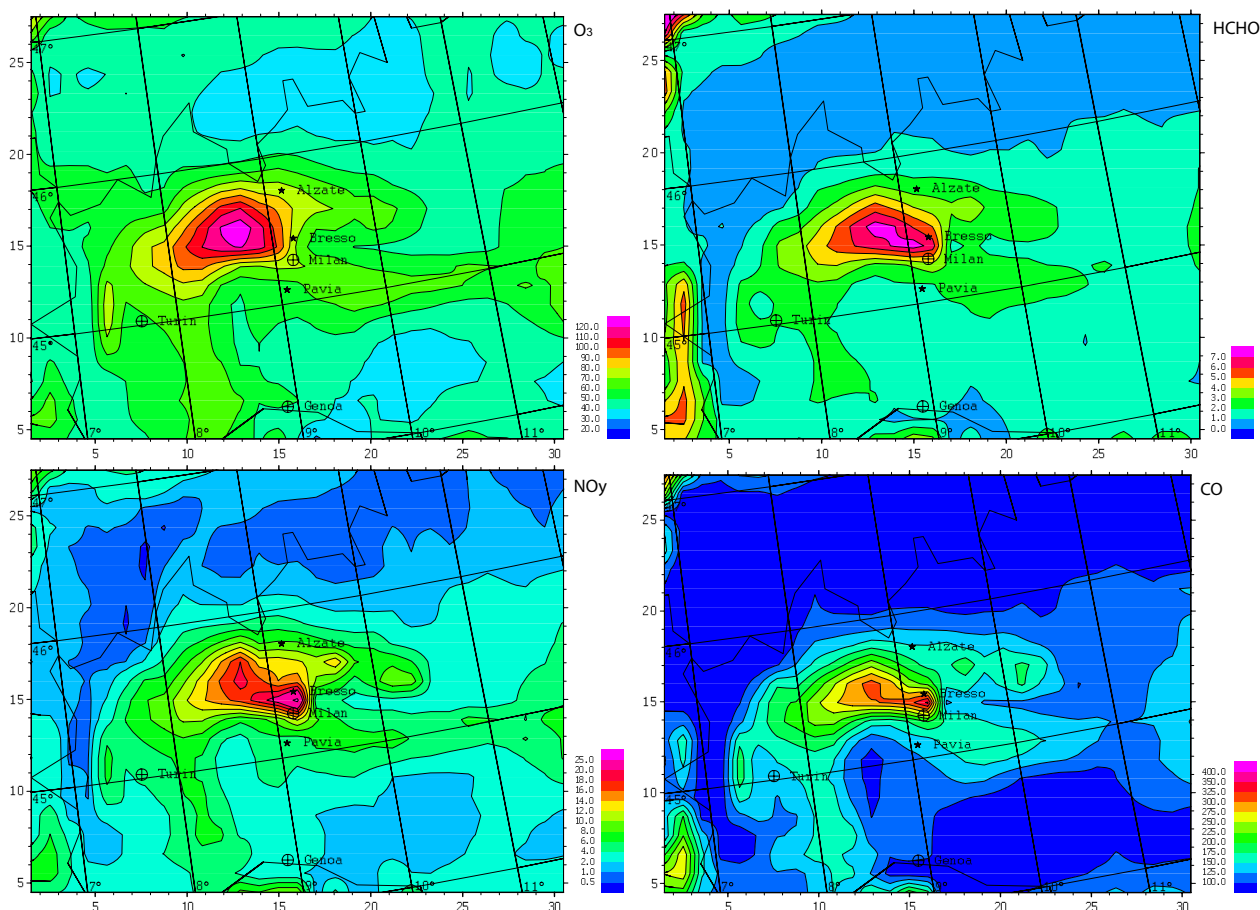


**Fig. 11.** Spatial distribution of  $\text{O}_3$ , HCHO,  $\text{NO}_y$  and CO in the Po Basin, at 14:00 on 17 August. The numbers marked outside of the frames show the number of grid cells (15 km for each grid size). The longitude/latitude are marked inside of the frame. The aircraft captured the highest ozone level above 120 ppb in areas northwest of Milan city. The model results show good agreement with aircraft data.

5 ppb (Fig. 9), which agrees well with the aircraft measurements made at about 300 m.

The modelled spatial distributions and levels of  $\text{O}_3$ , HCHO,  $\text{NO}_y$  and CO in the Po Basin close to the surface at 14:00 h on 17 August are shown in Fig. 11. The 2 ppb HCHO contour (lower left panel) is covering a large area. This is caused by secondary formaldehyde produced by the oxidation of both anthropogenic and biogenic VOC emissions. The upper and lower right panels of Fig. 11 show the distribution of  $\text{NO}_y$  and CO, respectively. Close to the surface, the spatial distribution of total reactive nitrogen  $\text{NO}_y$  reflects the combined influence of the emissions and transport.  $\text{NO}_y$  levels were about 15–20 ppb downwind of Milan. Inside and in the immediate vicinity of Milan (including Bresso) the  $\text{NO}_y$  mixing ratio was above 20 ppb. CO can be used as a tracer of emissions because of its long lifetime. CO levels up to 400 ppb were found in the city of Milan, and about 300 ppb of CO was observed inside the urban plume. This is low compared to the 850 ppb measured inside the plume on a day

in May 1998 (Thielmann et al., 2002). The measured plume was located east of  $9^\circ \text{E}$  (Fig. 10), and the modelled plume was further to the west (Fig. 11). Since there was no aircraft data available west of  $9^\circ \text{E}$ , it is difficult to assess the real width of the plume in this case. The difference between the modelled plume and only partly measured locations of the urban plumes seems to be due to the differences between the modelled and real wind directions. The modelled winds were from southeast, and the data was updated every 3 h. The measured winds were mainly from the southeast as well, but were sometimes from the south. The underestimated  $\text{O}_3$  and HCHO levels on 17 August shown in Fig. 9 can therefore be explained by the fact that the flight track is to the east of the modelled plume but partly inside the real plume. Dommen et al. (2002) suggested that downwind of the Milan metropolitan area, a regional plume was 50 km wide and atop of this the urban plume was 10–15 km wide. They also concluded that the background ozone levels in the Po Basin for those days were around 80–130 ppb, ozone levels were 15–30 ppb

higher in the regional plume, and the urban plume added another 10–30 ppb. Therefore, the difference in O<sub>3</sub> mixing ratios between the urban plume and the surroundings was about 45–60 ppb in 50 km distance. Our model produces an urban plume of about 15–20 km width, with O<sub>3</sub> mixing ratios about 40–50 ppb higher than outside the regional plume. The measured urban plume on 17 August in 2002 is about 10 km wide, and the levels are similar to our model results. The ozone gradients in the area north of Milan result from both anthropogenic and biogenic emissions. The comparison shows that the model is able to reproduce the O<sub>3</sub> mixing ratios in background air and in the photochemically produced urban plume reasonably well.

## 5 Conclusions

The NILU RCTM model has been applied to reproduce the photochemical evolution over the Milan metropolitan area during the FORMAT summer campaign of 2002, which took place between 22 July and 20 August. The model results were evaluated with measurements from two surface sites and aircraft data. The comparison shows that the time variation agrees well with the measurements both at urban and semi-rural sites. The discrepancies for CO and NO<sub>2</sub> are mainly caused by local sources at Bresso, which are not identified in the model. The underestimated CO and NO<sub>2</sub> levels at Alzate possibly are due to model resolution. The ozone peak values are well reproduced by the model. Both model results and measurements show low background O<sub>3</sub> levels of about 35 ppb during the 2002 campaign. The low O<sub>3</sub> levels can be ascribed to the low emissions in August and unstable weather conditions. The slopes of O<sub>3</sub> versus NO<sub>x</sub> of 5.1 and 4.9 are calculated from model results and measurements at Alzate, respectively. This indicates that the model has a reasonable representation of the ozone chemistry.

As the main target of the FORMAT project, HCHO was intensively measured during the campaign period with various techniques. The modelled HCHO has been evaluated with data from different instruments. At the semi-rural site Alzate, the model results were compared with data from both an in-situ instrument (Hantzsch) and a remote sensor (LP-DOAS). The measured HCHO from these two instruments shows large differences during fair weather days. The HCHO measured by LP-DOAS are sometimes twice the levels measured by the Hantzsch instrument. Local natural VOC emissions can explain the differences, because the light path of the LP-DOAS passed over a forest with strong isoprene emissions leading to fast HCHO formation, in particular on sunny days. In this case, the model results are close to the in-situ measurements, since both of them represent the general conditions of this location (forests are sparse in the Po basin). The scatter plot of HCHO versus (O<sub>3</sub> × water vapour) also indicates that the model and the in-situ instrument are representing similar air masses and photochemistry, while the LP-

DOAS is measuring a different air mass with higher VOC concentrations. This comparison demonstrates the importance of the experimental configuration since different instrumental setups can, depending on the surroundings, lead to highly different measurements. In-situ and remote sensing equipment, even when they are set up at the same location, are very often sampling air parcels with different contents of HCHO. When comparing the model results with measurements, not only the uncertainties have to be considered when comparing the measurements from different instruments, but it is also necessary to take into account how representative model results are when compared to point-measurements. With a 15 km × 15 km horizontal resolution, the model results represent an average situation over the grid box, whereas the point measurements represent the situation at a specific location. This is particularly important for measurements at polluted locations such as Bresso. This is why we focus more on the comparison with the Alzate data because we cannot expect that the model with 15 km horizontal resolution can reproduce the concentrations at a rather polluted site like Bresso perfectly.

The comparison with aircraft data shows that both the aircraft and model captured the plume on 17 August. Because of multi-day ozone build up, this was the day that both the model and the measurements show the ozone peaks with values above 120 ppb downwind of the Milan area. The measured plume was both observed and simulated northwest of Milan between 13:00 h to 14:00 h local time, about 30 km away from the city. The model results agree well with the aircraft measurements although the location of the modelled plume was slightly west of the real plume. This shift is caused by the wind data used in the model, since the wind blows from the southeast in the model, whereas it was blowing from the south-southeast in reality. There are some aspects in which the model simulation might be improved in the future. Model runs with higher horizontal resolution are needed. Since no HCHO emissions are included in this model, future modelling studies should include these emissions and sensitivity studies should be performed to quantify the contributions of primary and secondary HCHO. Higher resolution and more detailed land use data are needed for more specific information on biogenic emissions in this area. This is especially important for isoprene emissions, which depend on the forest type and solar radiation.

Edited by: T. Röckmann

## References

- Alicke, B. and Platt, U.: Impact of nitrous acid photolysis on the total hydroxyl radical budget during the Limitation of Oxidant Production/Pianura Padana Produzione di Ozono study in Milan, *J. Geophys. Res.*, 107(D22), 8196, doi:10.1029/2000JD000075, 2002.

- Andreani-Aksoyoglu, S., Prévôt, A. S. H., Baltensperger, U., Keller, J., and Dommen, J.: Modeling of formation and distribution of secondary aerosols in the Milan area (Italy), *J. Geophys. Res.*, 109, D05306, doi:10.1029/2003JD004231, 2004.
- Anfossi D., Sandroni S., and Viarengo S.: Tropospheric ozone in the nineteenth century: The Moncalieri series, *J. Geophys. Res.*, 96, 17 349–17 352, 1991.
- Baertsch-Ritter, N., Prévôt, A. S. H., Dommen, J., Andreani-Aksoyoglu, S., and Keller, J.: Model study with UAM-V in the Milan area (I) during PIPAPO: simulation with changed emissions compared to ground and airborne measurements, *Atmos. Environ.*, 37, 4133–4147, 2003.
- Baertsch-Ritter, N., Keller, J., Dommen, J., and Prévôt, A. S. H.: Effects of various meteorological conditions and spatial emission resolutions on the ozone concentration and ROG/NO<sub>x</sub> limitation in the Milan area (I), *Atmos. Chem. Phys.*, 4, 423–438, 2004, <http://www.atmos-chem-phys.net/4/423/2004/>.
- Berge, E.: Transboundary air pollution in Europe, Part 1, EMEP MSC-W Report 1/97, Norwegian Meteorological Institute, Oslo, 108 pp., 1997.
- Bott, A.: A positive definite advection scheme obtained by nonlinear renormalization of the advective fluxes, *Mon. Wea. Rev.*, 117, 1006–1015, 1989.
- Chameides, W. L., Lindsay, R. W., Richardson, J., and Kiang, C. S.: The role of biogenic hydrocarbons in urban photochemical smog: Atlanta as a case study, *Science*, 241, 1473–1475, 1988.
- Cárdenas, L. M., Brassington, D. J., Allan, B. J., Coe, H., Alicke, B., Platt, U., Wilson, K. M., Plane, J. M. C., and Penkett, S. A.: Intercomparison of formaldehyde measurements in clean and polluted atmosphere, *J. Atmos. Chem.*, 37, 53–80, 2000.
- Dommen, J., Prévôt, A. S. H., Neisinger, B., and Baumel, M.: Characterization of the photooxidant formation in the metropolitan area of Milan from aircraft measurements, *J. Geophys. Res.*, 107(D22), doi:10.1029/2000JD000283, 8197, 2002.
- Flatøy, F. and Hov, Ø.: Three-dimensional model studies of exchange processes of ozone in the troposphere over Europe, *J. Geophys. Res.*, 100, 11 465–11 481, 1995.
- Flatøy, F. and Hov, Ø.: Three-dimensional model studies of the effect of NO<sub>x</sub> emissions from aircraft on ozone in the upper troposphere over Europe and the North Atlantic, *J. Geophys. Res.*, 101, 1401–1422, 1996.
- Flatøy, F., Hov, Ø., and Schlager, H.: Chemical forecasts used for measurement flight planning during POLINAT 2, *Geophys. Res. Lett.*, 27, 951–954, 2000.
- Forrer, J., Ruttimann, R., Schneiter, D., Fischer, A., Buchmann, B., and Hofer, P.: Variability of trace gases at the high-Alpine site Jungfraujoch caused by meteorological transport processes, *J. Geophys. Res.*, 105, 12 241–12 251, 2000.
- Fried, A., Sewell, S., Henry, B., Wert, B. P., Gilpin, T., and Drummond, J. R.: Tunable diode laser absorption spectrometer for ground-based measurements of formaldehyde, *J. Geophys. Res.*, 102(D5), 6253–6266, 1997.
- Gilpin, T., Apel, E., Fried, A., Wert, B., Calvert, J., Genfa, Z., Dasgupta, P., Harder, J. W., Heikes, B., Hopkins, B., Westberg, H., Kleindienst, T., Lee, Y.-N., Zhou, X., Lonneman, W., and Sewell, S.: Intercomparison of six ambient [CH<sub>2</sub>O] measurement techniques, *J. Geophys. Res.*, 102, 21 161–21 188, 1997.
- Gong, H., Bradley, P. W., Simmons, M. S., and Tashkin, D. P.: Impaired exercise performance and pulmonary function in elite cyclists during low-level ozone exposure in a hot environment, *Am. Rev. Respir. Dis.*, 134, 726–733, 1986.
- Grønås, S., Foss, A., and Lystad, M.: Numerical simulation of polar lows in the Norwegian sea, *Tellus*, 39A, 334–353, 1987.
- Hak, C., Pundt, I., Trick, S., Kern, C., Platt, U., Dommen, J., Ordóñez, C., Prévôt, A. S. H., Junkermann, W., Astorga-Lloréns, C., Larsen, B. R., Mellqvist, J., Strandberg, A., Yu, Y., Galle, B., Kleffmann, J., Lörzer, J. C., Braathen, G. O., and Volkamer, R.: Intercomparison of four different in-situ techniques for ambient formaldehyde measurements in urban air, *Atmos. Chem. Phys.*, 5, 2881–2900, 2005, <http://www.atmos-chem-phys.net/5/2881/2005/>.
- Harris, G. W., Mackay, G. I., Iguchi, T., Mayne, L. K., and Schiff, H. I.: Measurements of formaldehyde in the troposphere by tunable diode laser absorption spectroscopy, *J. Atmos. Chem.*, 8, 119–137, 1989.
- Hass, H.: Description of the EURAD Chemistry-Transport-Model Version 2 (CTM2), Heft 83, Institut für Geophys. und Meteorologie, University of Cologne, Germany, 1991.
- Heck, W. W., Taylor, O. C., Adams, R., Bingham, G., Miller, J., Preston, E. and Weinstein, L.: Assessment of crop loss from ozone, *J. Air Pollut. control Assoc.*, 32, 353–361, 1982.
- Heikes, B., McCully, B., Zhou, X., Lee, Y.-N., Mopper, K., Chen, X., Mackay, G., Karecki, D., Schiff, H., Campos, T., and Atlas, E.: Formaldehyde methods comparison in the remote lower troposphere during the Mauna Loa Photochemistry Experiment, *J. Geophys. Res.*, 101, 14 741–14 755, 1996.
- Hov, Ø., Eliassen, A., and Simpon, D.: Calculation of the distribution of NO<sub>x</sub> compounds in Europe, in: *Tropospheric ozone*, edited by: Isaksen, I.S.A., pp. 239–261, Reidel D., Norwell Mass., 1988.
- Hov, Ø. and Flatøy, F.: Convective redistribution of ozone and oxides of nitrogen in the troposphere over Europe in summer and fall, *J. Atmos. Chem.*, 28, 319–337, 1997.
- Isaksen, I. S. A., Hov, Ø., and Hesstvedt, E.: Ozone generation over rural areas, *Environ. Sci. Technol.*, 12, 1279–1284, 1978.
- Junkermann, W. and Burger, J. M.: A new portable instrument for continuous measurement of formaldehyde in ambient air, *J. Atmos. Oceanic Technol.*, 23(1), 38–45, 2006.
- Kelly, T. J. and Fortune, C. R.: Continuous monitoring of gaseous formaldehyde using an improved fluorescence approach, *Int. J. Environ. Anal. Chem.*, 54, 249–263, 1994.
- Lawson, D. R., Biermann, H. W., Tuazon, E. C., Winer, A. M., Mackay, G. I., Schiff, H. I., Kok, G. L., Dasgupta, P. K., and Fung, K.: Formaldehyde measurement methods evaluation and ambient concentrations during the Carbonaceous Species Methods Comparison Study, *Aerosol Sci. Technol.*, 12, 64–76, 1990.
- Lee, Y.-N. and Zhou, X.: Method for the determination of some soluble atmospheric carbonyl compounds, *Environ. Sci. Technol.*, 27, 749–756, 1993.
- Lin, X., Trainer, M., and Liu, S. C.: On the nonlinearity of the tropospheric ozone production, *J. Geophys. Res.*, 93, 15 879–15 888, 1988.
- Liu, S. C., Trainer, M., Fehsenfeld, F. S., Parrish, D. D., Williams, E. J., Fahey, D. W., Hubler, G., and Murphy, P. C.: Ozone production in the rural troposphere and implications for regional and global ozone distributions, *J. Geophys. Res.*, 92, 4191–4207, 1987.
- Lübker, B. and Schöpp, W.: A Model to Calculate Natural VOC



- Emissions from Forests in Europe, International Institute for Applied Systems Analysis, A-2361, Laxenburg, Austria, 1989.
- Mckeen, S. A., Hsie, E.-Y., Trainer, M., Tallamraju, R., and Liu, S. C.: A regional model study of the ozone budget in the eastern United States, *J. Geophys. Res.*, 96, 10 809–10 845, 1991.
- Marengo, A., Gouget, H., Nédélec, P., Pagés, J.-P., and Karcher, F.: Evidence of a long-term increase in tropospheric ozone from Pic du Midi data series: Consequences: Positive radiative forcing, *J. Geophys. Res.*, 99(D8), 16 617–16 632, 1994.
- Martilli, A., Neftel, A., Favaro, G., Kirchner, F., Sillman, S., and Clappier, A.: Simulation of the ozone formation in the northern part of the Po Valley, *J. Geophys. Res.*, 107(D22), 8195, doi:10.1029/2001JD000534, 2002.
- Neftel, A., Spirig, C., Prévôt, A. S. H., Furger, M., Stutz, J., Vogel, B., and Hjorth, J.: Sensitivity of photooxidant production in the Milan Basin: An overview of results from a EUROTRAC-2 Limitation of Oxidant Production field experiment, *J. Geophys. Res.*, 107(D22), doi:10.1029/2001JD001263, 8188, 2002.
- Nordeng, T. E.: Parameterization of physical processes in a three-dimensional numerical weather model, Techn. Rep. 65, Norw. Meteorol. Inst., Oslo, 1986.
- Ordóñez, C., Mathis, H., Furger, M., Henne, S., Hüglin, C., Staehelin, J., and Prévôt, A. S. H.: Changes of daily surface ozone maxima in Switzerland in all seasons from 1992 to 2002 and discussion of summer 2003, *Atmos. Chem. Phys.*, 5, 1187–1203, 2005, <http://www.atmos-chem-phys.net/5/1187/2005/>.
- Pavelin, E. G., Johnson, C. E., Rughooputh, S., and Toumi, R.: Evaluation of pre-industrial surface ozone measurements made using Schönbein's method, *Atmos. Environ.*, 33, 6, 919–929, 1999.
- Pluim, J. E. and Chang, J. S.: A non-local closure model for vertical mixing in the convective boundary layer, *Atmos. Environ.*, 26, 9919–9933, 1992.
- Prévôt, A. S. H., Staehelin, J., Kok, G. L., Schillawski, R. D., Neininger, B., Staffelbach, T., Neftel, A., Wernli, H., and Dommen J.: The Milan photooxidant plume, *J. Geophys. Res.*, 102, 23 375–23 388, 1997.
- Sillman, S. and Samson, P. J.: Impact of temperature on oxidant photochemistry in urban, polluted rural and remote environments, *J. Geophys. Res.*, 100(D6), 11 497–11 508, 1995.
- Solberg, S., Bergström, R., Langner, J., Laurila, T., and Lindskog, A.: Changes in Nordic surface ozone episodes due to European emission reductions in the 1990s, *Atmos. Environ.*, 39(1), 179–192, 2004.
- Solberg, S., Derwent, R. G., Hov, Ø., Langner, J., and Lindskog, A.: European abatement of surface ozone in a global perspective, *Ambio*, 34, 47–53, 2005.
- Staehelin, J., Thudium, J., Buehler, R., Volz-Thomas, A., and Graber, W.: Trends in surface ozone concentrations at Arosa (Switzerland), *Atmos. Environ.*, 28, 75–87, 1994.
- Staffelbach, T., Neftel, A., and Horowitz, L. W.: Photochemical oxidant formation over Southern Switzerland, part II: Model results, *J. Geophys. Res.*, 102, 23 363–23 374, 1997.
- Strand, A. and Hov, Ø.: A two dimensional global study of the tropospheric ozone production, *J. Geophys. Res.*, 99, 22 877–22 895, 1994.
- Steinbacher, M., Dommen, J., Ordóñez, C., Reimann, S., Staehelin, S., Andreani-Aksoyoglu, S., and Prévôt, A. S. H.: Volatile organic compounds in the Po Basin. Part B: biogenic VOCs, *J. Atmos. Chem.*, 51, 293–315, 2005.
- Thielmann, A., Prévôt, A. S. H., and Staehelin, J.: Sensitivity of ozone production derived from field measurements in the Italian Po basin, *J. Geophys. Res.*, 107(D22), 8194, doi:10.1029/2000JD000119, 2002.
- Tilmes, S., Brandt, J., Flatøy, F., Bergström, R., Flemming, J., Langner, J., Christensen, J. H., Frohn, L. M., Hov, Ø., Jacobsen, I., Stern, R., and Zimmermann, J.: Comparison of five Eulerian air pollution forecasting systems for the summer of 1999 using the German ozone monitoring data, *J. Atmos. Chem.*, 42, 91–121, 2002.
- Trainer, M., Williams, E. J., Parrish, D. D., Buhr, M. P., Allwine, E. J., Westberg, H. H., Fehsenfeld, F. G., and Liu, S. C.: Models and observations of the impact of natural hydrocarbons on rural ozone, *Nature*, 329, 705–707, 1987.
- Trainer, M., Parrish, D. D., Buhr, M. P., Norton, R. B., Fehsenfeld, F. C., Anlauf, K. G., Bottenheim, W. J., Tang, Y. Z., Wiebe, H. A., Roberts, J. M., Tanner, R. L., Newman, L., Bowersox, V. C., Meagher, J. F., Olszyna, K. J., Rodgers, M. O., Wang, T., Berresheim, H., Demerjian, K. L., and Roychowdhury, U. K.: Correlation of ozone within NO<sub>y</sub> in photochemically aged air, *J. Geophys. Res.*, 98(D2), 2917–2925, doi:10.1029/92JD01910, 1993.
- Van Aardenne, J. A., Dentener, F. J., Olivier, J. G. J., Goldewijk, K., and Lelieveld, J.: A 1 × 1 degree resolution dataset of historical anthropogenic trace gas emissions for the period 1890–1990, *Global Biogeochem. Cycles*, 15(4), 909–928, 2001.
- Volz, A. and Kley, D.: Evaluation of the Montsouris series of ozone measurements made in the nineteenth century, *Nature*, 332, 218–219, 1988.
- Weber, R. O. and Prévôt, A. S. H.: Climatology of ozone transport from the free troposphere into the boundary layer south of the Alps during North Foehn, *J. Geophys. Res.*, 107(D3), 4030, doi:10.1029/2001JD000987, 2002.
- White, J. U.: Very Long Optical Paths in Air, *J. Opt. Soc. Am.*, 66, 411–416, 1976.